

Original research article

Anticancer and antimicrobial evaluation of extract from brown algae *Hormophysa cuneiformis*

Nehal A. H. K. Osman¹, Omniya M. Abd-Elazeem², Rasha A. Al-Eisa³, Nahla S. El-Shenawy^{2*}

¹ Suez Canal University, Faculty of Science, Botany and Microbiology Department, Ismailia 41522, Egypt

² Suez Canal University, Faculty of Science, Department of Zoology, Ismailia 41522, Egypt

³ Taif University, College of Sciences, Department of Biology, Taif 21944, Saudi Arabia

Abstract

Aim: We investigated the antimicrobial and anticancer properties of an ethanol crude extract of Red Sea brown alga (*Hormophysa cuneiformis*) from Egypt.

Methods: Extraction was achieved by mixing 100 g of sample powder with absolute ethanol, incubating at 37 °C overnight in a shaking incubator, and then collecting the extract. The extract's antimicrobial activity was tested using a well diffusion assay against the tested pathogens (*Escherichia coli*, *Bacillus subtilis*, *Staphylococcus aureus*, and *Candida albicans*) in comparison to commercial antibiotics. Anticancer activity was assessed using MTT assay on MCF-7, HepG-2, and HEP-2 cell lines. The anticancer mechanism of action against the HepG-2 cell line was investigated using cell cycle analysis, Annexin V, and antioxidant enzymes, in addition to transmission electron microscopy.

Results: GC-MS phytoconstituent profile of the extract was dominant with fatty acids. A broad antimicrobial effect against all the pathogenic isolates of *E. coli*, *S. aureus*, *B. subtilis*, and *C. albicans* was demonstrated, especially at the high concentration in comparison to commercial antibiotics. The extract could inhibit the growth of the tested cell lines. We observed the most significant effect on HepG-2 cells, and the concentration of the extract played a role in the level of inhibition (IC_{50} of 44.6 ± 0.6 µg/ml). The extract had negligible effects on Vero normal cell lines at the lower concentration, with slight toxicity (90.8% viability) at the highest concentration (500 µg/ml). At this same concentration, the extract caused 80–92% inhibition of the cancer cell lines. The extract appears to have demonstrated promising effects on cancer cells. It induces programmed cell death (apoptosis), arrests the cell cycle, and affects the oxidative/antioxidant balance within the cells, potentially leading to the suppression or elimination of cancer cells. These findings are encouraging and may have implications for cancer treatment or further research in this area. More action of extract was seen against bacteria than fungi, with a wide antibacterial impact against all of the tested isolates, notably at the high concentration in comparison to conventional antibiotics.

Conclusion: According to the findings, *H. cuneiformis* may be a valuable source of chemicals that are both antimicrobial and anticancer.

Keywords: Anticancer; Antimicrobial; Antioxidant enzymes; Cell cycle; Electron microscope; *H. cuneiformis*, HepG-2 cell line

Highlights:

- Antimicrobial and anticancer activity of the ethanol extract of *H. cuneiformis*.
- The mechanism of the extract was found to be related to apoptosis and cell cycle arrest.
- The extract was found to affect the oxidative status of cancer cells.

Introduction

Microbial antibiotic resistance and cancer are two serious problems that our modern world is facing. The WHO reports that many commonly used antibiotics are losing their ability to combat bacteria. This leads to difficulties in treatment and controlling infections that can eventually lead to death – especially during surgeries such as cancer, cesarean, and transplantation (WHO, 2021). On the other hand, the second greatest cause of death worldwide is cancer (WHO, 2022). According to WHO, the most common cancer deaths in 2020 were lung,

colon, liver, stomach, and breast (WHO, 2022). Only a small proportion of patients may be candidates for surgery, depending on the type and stage of their cancer (Berry, 2014). Chemotherapy and radiation therapy are two other techniques that can be used in conjunction with surgery. However, these treatments may come with serious side effects, such as xerostomia, tiredness, diarrhea, and secondary cancers (Piroux et al., 2020). Based on this, the need to find new alternative solutions to work against these increasing problems is urgent. Natural products offer a dependable substitute when looking for chemicals that can help to prevent and treat diseases (Pádua et al., 2015; Wang et al., 2021). Natural products from marine

* **Corresponding author:** Nahla S. El-Shenawy, Suez Canal University, Faculty of Science, Zoology Department, Ismailia, 41522, Egypt; e-mail: elshenawy_nahla@hotmail.com; nahla_elshennawy@science.suez.edu.eg
<http://doi.org/10.32725/jab.2023.016>

Submitted: 2023-01-07 • Accepted: 2023-09-21 • Prepublished online: 2023-09-22

J Appl Biomed 21/3: 121–136 • EISSN 1214-0287 • ISSN 1214-021X

© 2023 The Authors. Published by University of South Bohemia in České Budějovice, Faculty of Health and Social Sciences.

This is an open access article under the CC BY-NC-ND license.

sources have received increasing coverage (Chamberlin et al., 2019). Among the most important marine studied sources, extracts and substances made from marine algae have promising antimicrobial, anticancer, antioxidant, and anti-inflammatory properties (Barreca et al., 2020).

The compounds found in marine algae are structurally distinct, with a wide range of pharmacological properties that are absent in terrestrial plants (Barzkar et al., 2019; Salehi et al., 2019). Flavonoids, fatty acids, fucoidan, alginate, fucoxanthin, phenolics, and other compounds may have unique health-promoting properties that might be exploited in human health-care applications, including microbes and cancer treatment (Mohamed and Saber, 2019). Several studies have reported marine algae and their compounds for their antimicrobial and anticancer activity (Biris-Dorhoi et al., 2020; Osman et al., 2019, 2020; Moga et al., 2021; Teleb et al., 2022). Egypt's Red Sea is full of valuable marine algae that still need to be investigated for their bioactivity (Osman et al., 2020). *Hormophyssa cuneiformis* is an abundant brown marine alga that blooms on the coral reefs of the Red Sea, especially when extensive expanses of dead coral are present (Rashad and El-Chaghaby, 2020). Yet, this alga is scarcely investigated for its bioactivity and chemical profiling (Mohamed and Saber, 2019; Osman et al., 2020; Rashad and El-Chaghaby, 2020). Therefore, this research aimed to look into the possible antimicrobial and anticancer properties of ethanol extract from the brown alga *H. cuneiformis* and having a chemical profile for its extract.

Materials and methods

Sample collection and extract preparation

H. cuneiformis, a brown alga, was collected from the intertidal and subtidal zones of Ras Sudr reefs, Red Sea, Egypt in March 2017. The sample was washed with seawater to remove any impurities and then washed with fresh water to remove excess salt. It was dried by air in the shade, then ground and stored in plastic bags until future use. Extraction was achieved by mixing 100 g of sample powder with absolute ethanol, incubating at 37 °C overnight in a shaking incubator, and then collecting the extract. The process was carried out three times or until no color was observed. The extract was then evaporated to dryness under a reduced pressure vacuum (after being filtered using Whatman No. 4 filter paper). For cell experiments, a 50 mg/ml stock solution was prepared by dissolving the crude extract in dimethyl sulfoxide (DMSO). DMSO was used to prepare the needed concentrations. For the antimicrobial experiment, the stock solution and different concentrations were prepared using absolute ethanol.

GC-MS phytoconstituent profiling of the extract

The Thermo Scientific TRACE 1310 gas chromatograph coupled with an IQS LT single quadrupole mass spectrometer was employed for *H. cuneiformis* ethanol crude extract analysis. This instrument (30 m length; 0.25 mm internal diameter; 0.25 film thickness) used a DB5-MS and a capillary column filled with cross-linked 5% diphenyl and 95% dimethylpolysiloxane. An electron ionization system was employed for GC/MS detection. It was ionized with a 70 eV energy. The carrier was made up almost entirely of helium gas. It had a 1 ml/min constant flow rate and a 1 ml injection volume (splitless mode; injector temperature, 200 °C; ion-source temperature, 300 °C). The oven was at a set temperature of 40 °C (isothermal for 3 min). It increased at a rate of 5 °C/min until it reached 280 °C, after which it increased at a rate of 7.5 °C/min

until it reached 290 °C. A 9-min isothermal at 300 °C marked the end of this phase. At 70 eV, mass spectra were recorded. Additionally, 0.5-second scan intervals and components between 45 and 450 Da were collected. The GC ran for 63 min in total. Mass spectra and chromatograms were processed using a TurboMass, and the relative percentage sum of each factor was calculated by multiplying its average peak area by the total number of areas.

Estimation of the extract's antimicrobial activity using well diffusion assay

The antimicrobial effect of *H. cuneiformis* extract was tested using the well-diffusion method (Behravan et al., 2019) against selected microorganisms. Standard isolates of *Bacillus subtilis* (ATCC 10783) (NRRL B-543) and *Staphylococcus aureus* (ATCC 25923) as gram-positive bacteria, *Escherichia coli* (ATCC 25922) as gram-negative bacteria, in addition to *Candida albicans* (ATCC 16404) as fungus were used. The isolates were acquired from the Botany and Microbiology Department, Faculty of Science, Suez Canal University, Egypt. On Muller Hinton agar and Sabouraud Dextrose Agar media, 100 µl of a solution containing 108 cfu/ml of bacteria and 106 cfu/ml of fungus, were applied, respectively. A sterile cork borer was used to create wells that were 6 mm in diameter. The wells were loaded with different concentrations of the extract at 25 µg/well and 50 µg/well. DMSO was used as a negative control at a concentration of 0.1%. For positive control, Augmentin (AG), Chloramphenicol (C), and Streptomycin (S) were used at 30 µg/well. The inoculated plates were incubated at 37 °C (24 h for bacteria and 48 h for the fungus). The size of the inhibition zone (mm) was measured and taken as an indication of antimicrobial action for the extract.

Evaluation of the extract's anticancer activity

Normal and cancer cell lines culture and maintenance

Normal Vero cells (monkey kidney), MCF-7 cells (human breast cancer cell line), HepG-2 cells (human hepatocellular cancer cell line), and HEP-2 cells (human larynx cancer cell line) were acquired, cultured, and maintained at the regional center of mycology and biotechnology (Al-Azhar University, Egypt). For Vero cell, Roswell Park Memorial Institute (RPMI) medium was used, accompanied by 1% antibiotic (100 U/ml of penicillin, 100 µg/ml of streptomycin), sodium pyruvate (110 mg/ml), and 10% FBS. On Dulbecco's modified Eagle's medium (DMEM), which also contains 10% heat-inactivated foetal bovine serum, 1% L-glutamine, a HEPES buffer, and 50 mg/ml gentamycin, cancer cells were cultured. Every cell line was subcultured twice weekly at 37 °C in 5% CO₂ (Mirabelli et al., 2019).

Extract cytotoxicity test against Vero normal cell line

The cytotoxicity of extracts was assessed using the colorimetric MTT test (Mosmann, 1983). Vero cells were sown in a 96-well plate at a density of 1×10^5 cells/ml and incubated there for 24 h at 37 °C and 5% CO₂. The cells were subsequently exposed to extract at various concentrations (62.5, 125, 250, and 500 µg/ml) and incubated for an additional 24 h. Following incubation, 250 µl of the MTT stock solution (50 µl; 2 mg/ml) was applied to each well. After 3 h of incubation, the supernatants were removed, and each well's formazan crystals were dissolved using DMSO. Using an ELISA microplate reader, the produced purple formazan's absorption was determined at 540 nm. 100% vitality was determined by the optical density (OD) of the formazan produced in the untreated control cells. The result is shown as the mean percentage of viable cells com-

pared to the corresponding control (Vijayarathna and Sasidharan, 2012).

Evaluation of extract proliferation inhibitory effect against cancer cell lines

MCF-7, HepG-2, and HEP-2 cancer cell lines were planted in a 96-well plate at a cell concentration of 1×10^5 cells/ml. After 24 h incubation (37 °C with 5% CO₂), each cell line was treated with different extract concentrations (3.9, 7.8, 15.6, 31.25, 62.5, 125, 250, and 500 µg/ml) and further incubated for 24 h. The inhibition in cancer cell line growth was measured using the MTT assay (Mosmann, 1983) as described above. The OD for control cells (no treatment) was considered to have 100% viability. The data are presented as the mean percentage of inhibition compared to the control group's inhibition of cell growth. The 50% inhibitory concentration (IC₅₀) was calculated for each cell line. The cancer cells most susceptible to the extract proceeded for further mechanism investigation.

Cell cycle analysis

To survey the proportion of DNA content and cytotoxicity mechanism of the extract, a cell cycle analysis was performed according to Nicoletti et al. (1991). HepG-2 cancer cells were seeded on 6-well plates with 2×10^5 cells/ml concentration and treated with the extract at various concentrations (25, 50, and 100 µg/ml). The cells were harvested after 24 h incubation (37 °C with 5% CO₂), fixed in 1 ml of 70% ethanol for 30 min at 4 °C, and rinsed twice via 2 mM EDTA in PBS (spin at 2000 rpm for 5 min per each wash), then incubated in the dark with 1ml propidium iodide (PI) solution composed of 2 mM EDTA PBS, 100 µg of (PI) and 100 µg RNaseA for 30 min at 37 °C. The percentage of cells at each cell cycle stage was calculated using flow cytometry (Tigu et al., 2021).

Analysis of apoptosis with Annexin V Staining

Annexin-V FITC assay kit was used to quantify early and late apoptosis, as well as necrosis for the extract-treated cancer cell line through a flow cytometer. The same procedures of treatment and cell preparation for cell cycle analysis were used. After rinsing twice with PBS, 500 µl of binding buffer was added. 5 µl of Annexin-V FITC and 5 µl of PI were used to stain the cells for 5 min at room temperature. The cells were analyzed using a flow cytometer to give a percentage of apoptotic and necrotic cells (Lakshmanan and Batra, 2013).

Estimation of oxidative status biomarkers

The oxidative stress biomarkers of the extract were evaluated by the determination of the oxidative stress products and antioxidant enzymes. HepG-2 cancer cells were seeded on 6-well plates with 2×10^5 cells/ml and treated with different concentrations of extract (25, 50, and 100 µg/ml). The cells were harvested after 24 h incubation (37 °C with 5% CO₂) and then lysed using ultrasonication in 0.1 M potassium phosphate buffer (pH 7.4) and 1.15% KCl for 1 min. Following a 15-minute centrifugation at 3000 rpm of the combination, the supernatant was utilized to measure the levels of oxidative enzymes.

Determination of malondialdehyde (MDA)

200 µl of supernatant was mixed with 1.5 ml of 0.8% 2-thio-barbituric acid and 1.5 ml of 20% acetic acid. A pink color was formed that was measured with a spectrophotometer at 532 nm. Using 1,1',3,3'-tetramethoxypropane serial dilutions, a calibration curve was created. The information was displayed as nmol/ml (Uchiyama and Mihara, 1978).

Determination of myeloperoxidase (MPO)

Hexadecyl trimethyl ammonium bromide was diluted 1 : 1 in 200 l of supernatant and then added to the mixture on ice. A tube containing 2 ml of chloroform was filled with the supernatant after the combination was centrifuged at 4000 rpm for 15 min at 4 °C. 1 ml of the top aqueous phase was taken shortly after, and it was centrifuged for 15 minutes at 8000 rpm. A mixture of 0.2 ml of supernatant, 0.5 ml of PBS, 0.6 ml of HBSS containing 0.25% bovine serum albumin, 0.1 ml of 0.125% DMB, and 0.1 ml of 0.05% H₂O₂ was created. After being vortexed, the mixture was let to stand at room temperature for 15 minutes. 0.5 ml of 1% sodium azide was added to stop the reaction, and the optical density (OD) was then measured spectrophotometrically at 460 nm as U/ml (Marklund, 1985).

Determination of Superoxide Dismutase (SOD)

25 µl of pyrogallol (24 mmol/l produced in HCl) were combined with 100 µl of supernatant, and the final volume was adjusted to 3 ml using Tris HCl (0.1 M, pH 7.8). The variations in absorbance were noted at 420 nm for 3 intervals, using a spectrophotometer. SOD was expressed as U/mg Protein (Marklund, 1985).

Determination of catalase (CAT)

100 µl of supernatant was mixed with 2.9 ml of 19 mmol/l H₂O₂ solutions prepared in potassium phosphate buffer (0.1 M, pH 7.4). A JANEWAY 6305 UV/Visible Spectrophotometer was used to record the changes in absorbance at 240 nm once per minute for two minutes. The enzyme was measured in U/mg proteins (Claiborne, 1985).

Determination of glutathione peroxidase (GPx)

200 µl of supernatant was mixed with 0.8 mM EDTA, 10 mM sodium azide, 2.5 mM H₂O₂, reduced glutathione, and 0.4 M phosphate buffer (pH 7). The mixture was incubated for 3 minutes at 37 °C before adding 0.5 ml of 10% TCA to terminate the process. The mixture was centrifuged at 2,000 rpm, and the supernatant was mixed with 3 ml of 0.3 mM disodium hydrogen phosphate and 1.0 ml of 0.04% DTNB. GPx was produced as U/mg proteins and the generated color was evaluated spectrophotometrically at 420 nm instantly (Paglia and Valentine, 1967).

Determination of glutathione-S-transferase (GST)

According to the GST kit, 500 µl of supernatant was mixed with 1 ml of phosphate buffer (pH 7.4) and 100 µl of glutathione reagent (GSH), and was then incubated for 5 min at 37 °C. A 100 µl of Chloro, 2dinitrobenzene (CDNB) was added to the mixture and again incubated for 5 min at 37 °C. The reaction was terminated using 100 µl trichloroacetic acid, and centrifuged at 3000 rpm for 5 min, then measured at 340 nm against the blank (Seyyedi et al., 2005). Results were expressed as nmol/mg proteins.

Determination of glutathione (GSH)

500 µl of supernatant was mixed with 500 µl TCA-EDTA, shaken for 15 min, then centrifuged for 5 min at 2000 rpm. 100 µl of supernatant was mixed with 1.7 ml phosphate buffer and 0.1 ml Ellman's reagent. A spectrophotometer was used to evaluate the optical density at 412 nm against a blank after five minutes using a GSH calibration curve. Proteins were used to measure GSH in mol/mg (Ellman, 1959).

Transmission electron microscopy

HepG-2 cells were seeded in 6-well plates at 1×10^5 cells/ml. After 24 h incubation, the cells were treated with the *H. cuneiformis* extract IC₅₀ (44.6 µg/ml) and incubated for another 24 h. The cells were rinsed in PBS before being fixed in a PBS buffer containing 2% paraformaldehyde and 2.5% glutaraldehyde. Before being anchored in 1% osmium tetroxide, the cells were washed twice in the same buffer. The cells were immersed in an LR White resin and polymerized after being rinsed and dehydrated in a graded alcohol series overnight at 70 °C. The ultrathin components were then chopped and put on a TEM grid using a diamond cutter. Using a Philips CM10 electron microscope with an 80 kV accelerating voltage, the bits were analyzed (Graham and Orenstein, 2007).

Data analysis

SPSS statistical package (SPSS Inc., Version 11.5) and Microsoft Excel 2010 were used for statistical analyses. ANOVA was used to test the significance of differences among treatments. Duncan's test was used for calculating the least significant differences among means at a probability level of $P \leq 0.05$. The IC₅₀ value was calculated as the *H. cuneiformis* ethanol extract concentration that inhibits cell proliferation by 50% compared to the untreated control cells. It was estimated from graphic plots of the concentration-response curve for each concentration using GraphPad Prism software (San Diego, CA, USA).

Results and discussion

GC-MS profile of the extract

The ethanol extract's phytochemical GC-MS analysis of *H. cuneiformis* (Fig. 1) revealed the existence of 49 compounds (36 of them shown in Table 1). Most of the compounds belonged to fatty acids with the presence of phthalic acid, phytol, terpenes, ketones as well as steroids. The saturated fatty acids were represented by palmitic (C16:0), myristic (C14:0), margaric acid (C17:0), and stearic (C18:0), with a peak area percentage of 29.12%, 3.91%, 27.87%, and 1.43%, respectively. Concerning monounsaturated fatty acids, oleic (C18:1, ω -9) acid was present with a peak area of 13.36%. Polyunsaturated fatty acids were dominant with arachidonic acid (C20:4, ω -6), alpha-linolenic acid (C18:3, ω -3), linoleic acid (C18:2, ω -6), eicosapentaenoic acid (C20:5, ω -3), dihomo- γ -linolenic (C20:3, ω -6), and docosahexaenoic acid (C22:6, ω -3). The current results are aligned with those of Mohamed and Saber (2019), who investigated *H. cuneiformis* chloroform extract collected from Hurghada, Egypt. In Table 2, the previous reports about the antimicrobial and anticancer activity of some compounds found in the *H. cuneiformis* crude ethanolic extract's profile were traced. The reports suggested 29 compounds in the ethanol extract of *H. cuneiformis* with antimicrobial and anticancer effects.

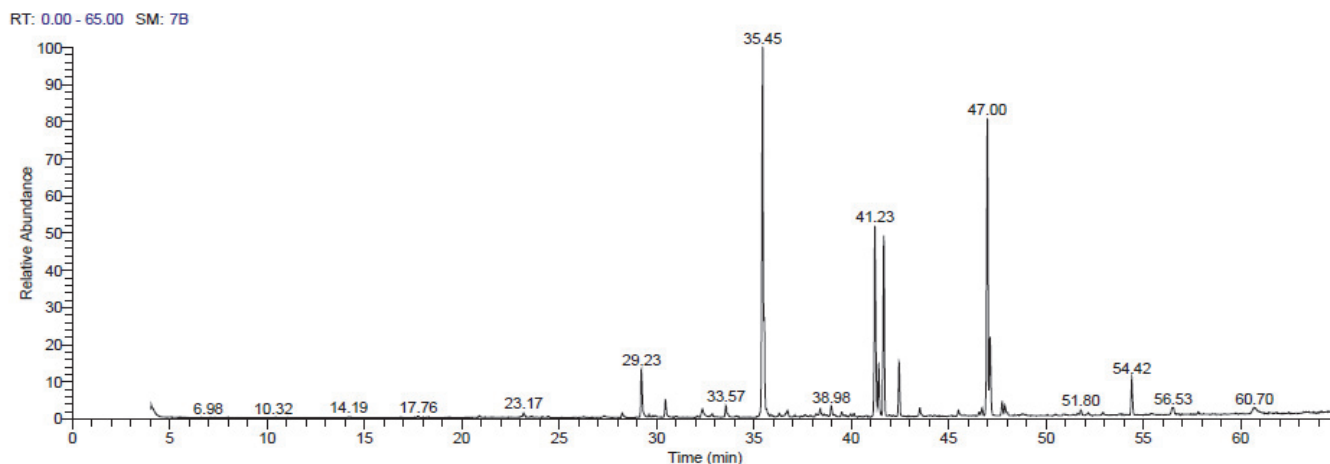


Fig. 1. GC-MS chromatogram of the absolute ethanol extract of *H. cuneiformis*

Antimicrobial activity

Researchers are studying new compounds to combat microbial resistance. In a step toward facing the problem of microbial resistance, novel compounds with antimicrobial effects have been a concern of researchers lately. Many publications have reported marine algal extracts as a valuable source of compounds that possess antimicrobial activity with fewer side effects and higher bioavailability in humans (Arguelles and Sapin, 2022; Biris-Dorhoi et al., 2020; Chojnacka et al., 2012; El Shafay et al., 2016; Mohamed and Saber 2019; Osman et al., 2019; Silva et al., 2020). In the current study, pathogenic isolates of *E. coli*, *S. aureus*, *B. subtilis*, and *C. albicans* were used to assess the antibacterial efficacy of *H. cuneiformis* ethanol extract. The results showed a broad antimicrobial effect against all the tested isolates, especially at the high concentration in comparison to commercial antibiotics (Table 3). The extract showed higher activity against bacteria than fungi. At the lower concentration (25 µg/well), the effect against the three bacterial isolates

(*E. coli*, *S. aureus*, and *B. subtilis*) had no significant difference. The extract at the higher concentration (50 µg/well) was noticed to be more effective against *S. aureus* and *B. subtilis* than *E. coli*, with the highest effect against *S. aureus*. The 50 µg/well extract concentration was found to possess an effect that is like or even higher than the tested commercial antibiotics. The results suggest that *H. cuneiformis* has the potential for use in developing new antibiotic drugs. The new results were better than those that Osman et al. (2019) reported. The current result about *C. albicans* was found to be lower than the one obtained by Mohamed and Saber (2019), who studied the effect of *H. cuneiformis* chloroform extract on fungi. Extracting solvent, the season of collection, and geography were found to affect the algal species activity (Osman et al., 2019), which explains the difference in results. As shown in Table 2, many of the extracts' analyzed compounds had been previously reported for their antimicrobial activity.

Table 1. Phyto-constituents profile for the ethanol extract of *H. cuneiformis* using GC-MS analysis

No	Compounds identified	RT	Peak area (%)	Mol. formula	Mol. Wt.
1	Hexadecanoic acid, Ethyl Ester	35.45	27.02	C ₁₈ H ₃₆ O ₂	284
2	Heptadecanoic acid, Ethyl Ester	35.45	27.02	C ₁₉ H ₃₈ O ₂	298
3	Ethyl Pentadecanoate	35.45	27.02	C ₁₇ H ₃₄ O ₂	270
4	5,8,11,14-Eicosatetraenoic acid, Ethyl Ester, (All-Z)-	47.00	19.08	C ₂₂ H ₃₆ O ₂	332
5	5,8,11,14-Eicosatetraenoic acid, Methyl Ester, (All-Z)-	47.00	19.08	C ₂₁ H ₃₄ O ₂	318
6	Ethyl Oleate (9-Octadecenoic acid (Z)-Ethyl Ester)	41.23	13.02	C ₂₀ H ₃₈ O ₂	310
7	Ethyl (9z,12z)-9,12-Octadecadieno Ate #	41.68	11.28	C ₂₀ H ₃₆ O ₂	308
8	9,12-Octadecadienoic acid, Methyl Ester, (E, E)-	41.68	11.28	C ₁₉ H ₃₄ O ₂	294
9	8,11,14-Eicosatrienoic acid, (Z,Z,Z)-	47.14	5.14	C ₂₀ H ₃₄ O ₂	306
10	9,12,15-Octadecatrienoic acid, Ethyl Ester, (Z,Z,Z)-	47.14	5.14	C ₂₀ H ₃₄ O ₂	306
11	9,12,15-Octadecatrienoic acid, Methyl Ester, (Z,Z,Z)-	47.14	5.14	C ₁₉ H ₃₂ O ₂	292
12	Tetradecanoic acid, Ethyl Ester	29.23	3.21	C ₁₆ H ₃₂ O ₂	256
13	1,2-Benzenedicarboxylic acid, disooctyl Ester	54.42	2.50	C ₂₄ H ₃₈ O ₄	390
14	1,2-Benzenedicarboxylic acid, 3-Nitro-	54.42	2.50	C ₈ H ₅ NO ₆	211
15	1,2-Benzenedicarboxylic acid, Mono(2-Ethylhexyl) Ester	54.42	2.50	C ₁₆ H ₂₂ O ₄	278
16	2-Pentadecanone, 6,10,14-Trimethyl-	30.46	1.21	C ₁₈ H ₃₆ O	268
17	2-Undecanone, 6,10-Dimethyl-	30.46	1.21	C ₁₃ H ₂₆ O	198
18	4,7,10,13,16,19-Docosahexaenoic acid, methyl ester, (all-Z)-	47.76	0.96	C ₂₃ H ₃₄ O ₂	342
19	Ethyl 5,8,11,14,17 icosapentaenoate	47.76	0.96	C ₂₂ H ₃₄ O ₂	330
20	5,8,11,14,17-Eicosapentaenoic acid, methyl ester, (all-Z)-	47.76	0.96	C ₂₁ H ₃₂ O ₂	316
21	5,8,11,14-Eicosatetraenoic acid, ethyl ester, (all-Z)-	47.76	0.96	C ₂₂ H ₃₆ O ₂	332
22	9,12,15-Octadecatrien-1-ol, (Z,Z,Z)-	47.91	0.88	C ₁₈ H ₃₂ O	264
23	Z,Z,Z-4,6,9-Nonadecatriene	47.91	0.88	C ₁₉ H ₃₄	262
24	Hexadecanoic acid, methyl ester	33.57	0.85	C ₁₇ H ₃₄ O ₂	270
25	Heptadecanoic acid, methyl ester	33.57	0.85	C ₁₈ H ₃₆ O ₂	284
26	Oxalic acid, mono-{5-[(2-bromophenyl)(2,2-dimethylpropionyloxy)methyl]-7,8-dihydro-5H-[1,3]dioxolo[4,5-g]isoquinolin-6-yl} ester	56.52	0.84	C ₂₄ H ₂₆ BrNO ₈	535
27	Octadecanoic acid, Ethyl Ester	56.52	0.84	C ₂₀ H ₄₀ O ₂	312
28	2-Myristynoyl pantetheine	56.52	0.84	C ₂₅ H ₄₄ N ₂ O ₅ S	484
29	Phytol	38.98	0.80	C ₂₀ H ₄₀ O	296
30	Ethyl iso-allocholate	60.69	0.74	C ₂₆ H ₄₄ O ₅	436
31	Ergosta-14,22-DIEN-3-OL, (3à,5à,22E)-	60.69	0.74	C ₂₈ H ₄₆ O	398
32	Allopregnane-3à,7à,11à-triol-20-one	60.69	0.74	C ₂₁ H ₃₄ O ₄	350
33	Methyl 10-oxohexadecanoate	43.54	0.70	C ₁₇ H ₃₂ O ₃	284
34	Z-8-Methyl-9-tetradecenoic acid	43.54	0.70	C ₁₅ H ₂₈ O ₂	240
35	9-Methyl-Z-10-tetradecen-1-ol acetate	43.54	0.70	C ₁₇ H ₃₂ O ₂	268
36	Dodecanoic acid, 11-oxo-, methyl ester	43.54	0.70	C ₁₃ H ₂₄ O ₃	228

Note: Compounds with a fatty-acid nature are in bold to show their dominance in the extract chemical profile.

Table 2. Previously reported antimicrobial and anticancer activity for some of the identified compounds in the ethanol extract of *H. cuneiformis*

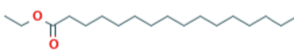

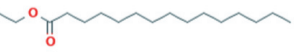
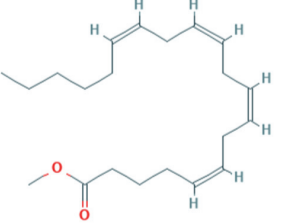

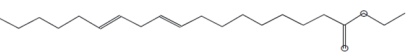
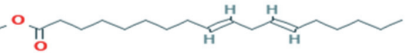
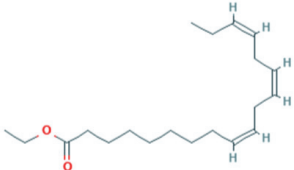
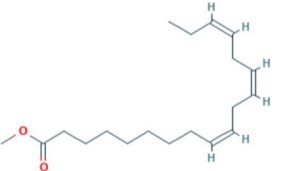
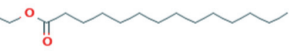
No	Name of the compound	Biological activity	References
1	Hexadecanoic Acid, Ethyl Ester 	Antioxidant, antimicrobial, anticancer activity, cancer preventive	Gideon, 2015; Guerrero et al., 2017; Jargalsaikhan et al., 2014; Sianipar and Purnamaningsih, 2016; Tyagi and Awargal, 2017; Zayed et al., 2014
2	Heptadecanoic Acid, Ethyl Ester 	Anti-microbial, antioxidant	Zayed et al., 2014
3	Ethyl Pentadecanoate 	Antimicrobial	Mujeeb et al., 2014
4	5,8,11,14-Eicosatetraenoic Acid, Methyl Ester, (All-Z)- 	Antifungal, antibacterial, antitumor cytotoxic effects	Agoramoorthy et al., 2007
5	Ethyl Oleate [9-Octadecenoic Acid (Z)-, Ethyl Ester] 	Anti-oxidative, anti proliferative, anti-cancer, anti-microbial	Abubakar and Majinda, 2016; Jargalsaikhan et al., 2014
6	Ethyl (9z,12z)-9,12-Octadecadieno Ate # 	Hepatoprotective	Guerrero et al., 2017; Tyagi and Awargal, 2017
7	9,12-Octadecadienoic Acid, Methyl Ester, (E, E) 	Antimicrobial, anticancer	El-Din and Mohyeldin, 2018
8	9,12,15-Octadecatrienoic Acid, Ethyl Ester, (Z,Z,Z)- 	Cancer preventive, hepatoprotective	Guerrero et al., 2017
9	9,12,15-Octadecatrienoic Acid, Methyl Ester, (Z,Z,Z)- 	Antimicrobial, Anticancer, Hepatoprotective, cancer preventive	Mujeeb et al., 2014; Tyagi and Awargal, 2017
10	Tetradecanoic Acid, Ethyl Ester 	Antioxidant, antimicrobial, cancer preventive	Gideon, 2015; Pinteus et al., 2017

Table 2. (continued)

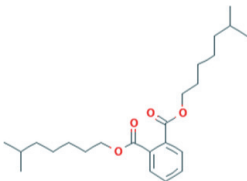
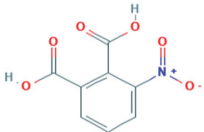
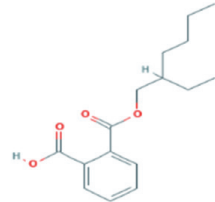
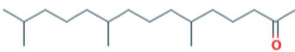

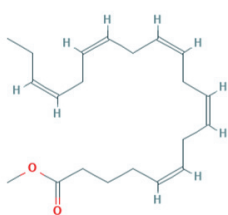
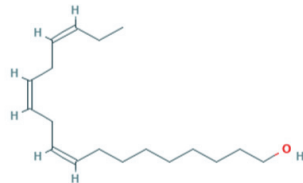
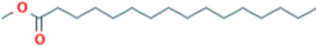

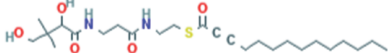
No	Name of the compound	Biological activity	References
11	1,2-Benzenedicarboxylic Acid, Diisooctyl Ester	Antimicrobial	Zayed et al., 2014
			
12	1,2-Benzenedicarboxylic Acid, 3-Nitro-	Antimicrobial, antioxidant	Elsayed et al., 2020
			
13	1,2-Benzenedicarboxylic Acid, Mono(2-Ethylhexyl) Ester	Antimicrobial, antioxidant	Beulah et al., 2018
			
14	2-Pentadecanone, 6,10,14-Trimethyl-	Antibacterial	Akpuaka et al., 2013; Yuyama et al., 2020
			
15	2-Undecanone, 6,10-Dimethyl-	Antibacterial	Reddy and Al-Rajab, 2016
			
16	5,8,11,14,17-Eicosapentaenoic acid, Methyl Ester, (all-Z)-	Cytotoxic	Rayssan and Shawkat, 2019
			
17	9,12,15-Octadecatrien-1-ol, (Z,Z,Z)-	Antimicrobial	Crout et al., 1982
			
18	Hexadecanoic Acid, Methyl Ester	Antifungal, antioxidant, antimicrobial	Akpuaka et al., 2013
			
19	Heptadecanoic Acid, Methyl Ester	Antioxidant	Zayed et al., 2014
			
20	2-Myristinoyl pantetheine	Antimicrobial	Marimuthu et al., 2014; Parham et al., 2020
			

Table 2. (continued)

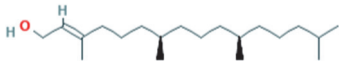
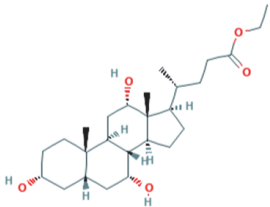
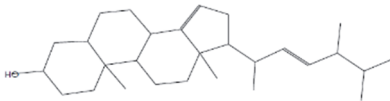
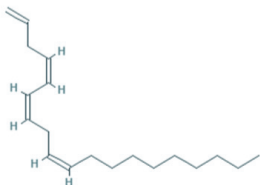
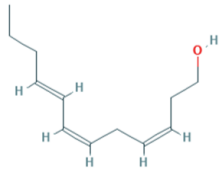
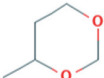
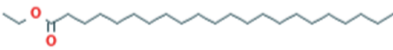
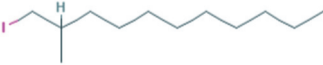
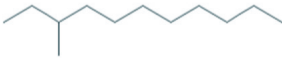
No	Name of the compound	Biological activity	References
21	Phytol 	Anticancer, antimicrobial	Rency et al., 2015; Seca and Pinto, 2018
22	Ethyl iso-allochololate 	Antimicrobial	Malathi and Ramaiah, 2017
23	Ergosta-14,22-Dien-3-OL, (3á,5à,22E)- 	Antimicrobial, antitumor	Ibrahim et al., 2020; Teixeira et al., 2019
24	Z,Z,Z-1,4,6,9-Nonadecatetraene 	Antimicrobial	Ibrahim et al., 2020
25	Z3, Z6, E8-Dodecatrien-1-OL 	Cytotoxicity, toxicity activity	Monzote et al., 2010; Pasaribu and Waluyo, 2020
26	1,3-Dioxane, 4-Methyl- 	Antibacterial, antifungal	Küçük et al., 2011; Shukla et al., 2018
27	Docosanoic Acid, Ethyl Ester 	Antibacterial, antioxidant	Gideon, 2015; Kim et al., 2020
28	1-Iodo-2-Methylundecane 	Antimicrobial	Nishanthini et al., 2014
29	Undecane, 3-Methyl- 	Antioxidant, antimicrobial	Mushtaq et al., 2013

Table 3. Antimicrobial activity of *H. cuneiformis* ethanol extract

Sample	Treatment	<i>E. coli</i>	<i>S. aureus</i>	<i>B. subtiles</i>	<i>C. albicans</i>
Negative control	Absolute ethanol	-ve	-ve	-ve	-ve
	AG	12 ^c ± 0.13	10 ^e ± 0.06	10 ^c ± 0.14	-ve
Positive control	C	11 ^d ± 0.07	17 ^c ± 0.09	15 ^b ± 0.03	18 ^a ± 0.07
	S	10 ^e ± 0.10	20 ^b ± 0.04	19 ^a ± 0.03	-ve
<i>H. cuneiformis</i>	25 µg/well	15 ^b ± 0.07	15 ^d ± 0.03	15 ^b ± 0.01	10 ^c ± 0.03
	50 µg/well	18 ^a ± 0.3	28 ^a ± 0.07	19 ^a ± 0.1	14 ^b ± 0.07

Note: Each value is the mean of the inhibition zone (mm) ± S.D (n = 3). AG, augmentin; C, chloramphenicol; S, streptomycin. Significance difference accepted at $P \leq 0.05$. Within the same column, values with different letters are significantly different.

Extract cytotoxicity against normal and cancer cells

As the second death-leading disease, cancer remains the concern of many scientists. The main goal for researchers in developing anticancer drugs is to seek more effective alternatives with fewer side effects. Marine macroalgae and their isolated compounds have been studied and reported for their anticancer effects (Biris-Dorhoi et al., 2020; Gupta and Abu-Ghannam, 2011; Gutiérrez-Rodríguez et al., 2018; Moga et al., 2021; Osman et al., 2020; Zorofchian Moghadamtousi et al., 2014). An MTT test was utilized in the current investigation to assess the cytotoxicity of *H. cuneiformis* on the viability percentage of healthy cells (Vero cell) and cancer cell lines (MCF-7, HepG-2, and HEP-2). The normal Vero cells showed a good adaptation to the different concentrations of *H. cuneiformis*, with slight cytotoxicity towards the high concentration (500 µg/ml had 90.8 % cell viability) (Fig. 2). For cancer cell lines, the extract was found to be effective in inhibiting the growth of the three cancer cell lines concentration-dependently (Table 4). The IC₅₀ values for the extract against MCF-7, HepG-2, and HEP-2 were 95 ± 3.9, 44.6 ± 0.6, and 156 ± 2.1 µg/ml, respectively (Table 4). The IC₅₀ results indicated the highest anticancer activity for the extract against HepG-2. These results agreed with the findings of Osman et al. (2020), who studied the anticancer activity of methanol extract of *H. cuneiformis* among six algal

extracts. Osman et al. (2020) found that *H. cuneiformis* had the highest anticancer activity against HL60, A549, and HCT116 cancer cells in a concentration-dependent manner. Many compounds discovered in the extract had been previously reported for their anticancer effect – as summarized in Table 2. As a result of being the most suppressed cancer cell line with *H. cuneiformis* extract, HepG-2 was chosen for further studies to understand the anticancer mechanism of the extract.

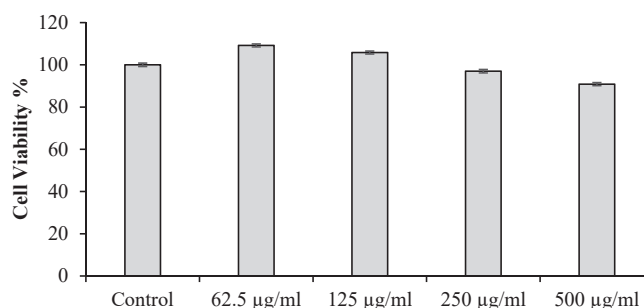


Fig. 2. Cytotoxicity effect of different extract concentrations (62.5, 125, 250, and 500 µg/ml) on Vero normal cell line versus control (untreated cells) using MTT assay to check cell viability %. Values are the mean of 3 replicas ± S.D.

Table 4. Growth inhibitory effect of *H. cuneiformis* extract at different concentrations against three cancer cell lines examined by MTT assay

Cell lines	Inhibitory effect (%) at different crude extract concentrations (µg/ml)								IC ₅₀ (µg/ml)
	3.9	7.8	15.6	31.25	62.5	125	250	500	
MCF-7	0	1.84 ^g ± 0.05	9.26 ^f ± 0.24	21.98 ^e ± 0.23	38.6 ^d ± 1.25	60.54 ^c ± 1.72	73.29 ^b ± 0.78	87.62 ^a ± 0.44	95 ± 3.9
HepG-2	5.77 ^h ± 0.11	11.49 ^g ± 0.21	25.18 ^f ± 0.54	43.25 ^e ± 0.76	59.02 ^d ± 0.72	71.68 ^c ± 0.84	84.03 ^b ± 0.34	92.48 ^a ± 0.24	44.6 ± 0.6
HEp-2	0	0	1.41 ^f ± 0.18	9.56 ^e ± 0.16	26.83 ^d ± 0.46	45.04 ^c ± 1.07	64.92 ^b ± 1.70	80.59 ^a ± 0.45	156 ± 2.1

Note: The values are the mean ± S.D (n = 3). $P \leq 0.05$ was accepted for significance deference. Values with different letters are significantly different.

Cell cycle analysis

To understand the anticancer mechanism of *H. cuneiformis* extract towards HepG-2 cancer cells, a flow cytometry analysis for the cell cycle stages was performed (Fig. 3). According to the results (Fig. 4), treatment with the extract was capable of significantly increasing the cells at the sub-G1 stage from 1.6% for the control (untreated) to 33.1% for the highest concentration (100 µg/ml). Accumulating cells at sub-G1 is an indication of apoptosis stimulation (Kajstura et al., 2007; Osman et al., 2020). The outcomes demonstrated a considerable concentration-dependent reduction in both G0-G1 and S phases upon extract treatment versus the control, indicating cell proliferation inhibition. For the G2-M phase, the results reflect a

significant elevation from 10.67% in the control to 35.3% at 100 µg/ml extract concentration. G2-M is a vital checkpoint for DNA damage in the cell cycle to decide whether to stop repairing DNA and proceed in proliferation or go through apoptosis. Shifting the cell population to the G2-M phase reflects a cell cycle arrest (Kajstura et al., 2007; Osman et al., 2020). Based on the results, the extract's anticancer effect is related to apoptosis stimulation as well as cell cycle arrest induction. This agrees with the results of Osman et al. (2020), who studied the mechanism of action of *H. cuneiformis* against HL60, A549, and HCT116 cancer cells. The results also agree with Sakthivel and Devi (2019), who studied the anticancer activity of related species *Hormophysa triquetra*.

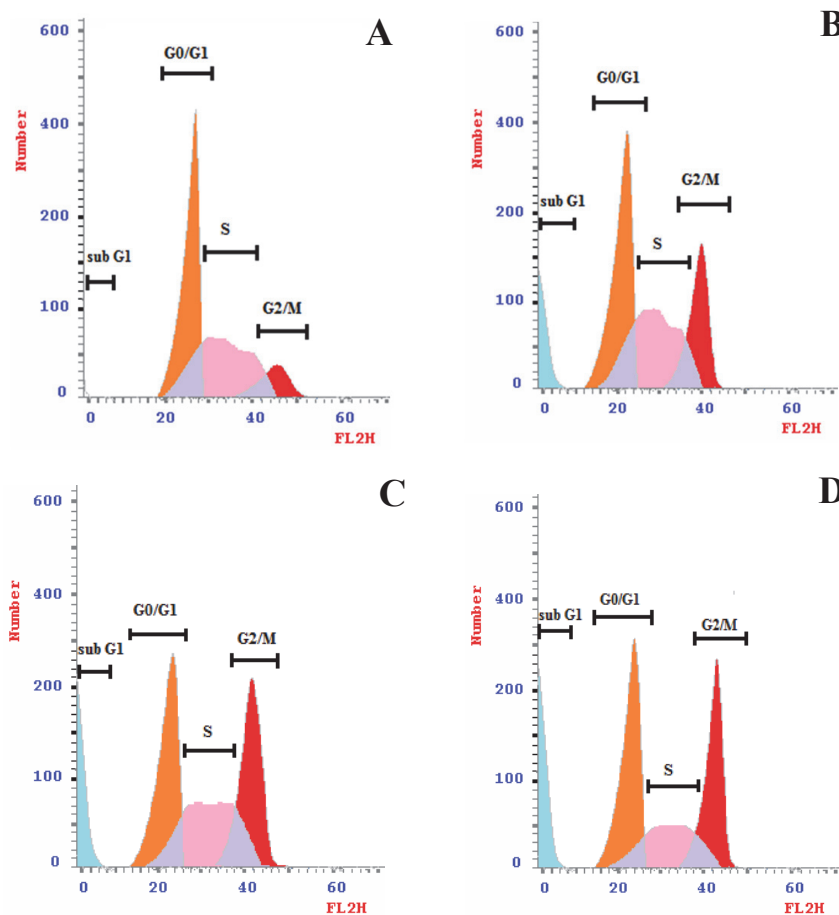


Fig. 3. Flow cytometric cell cycle analysis of propidium iodide (PI)-stained HepG-2 cells. HepG-2 cells were treated with different concentrations of *H. cuneiformis* ethanol extract (A = control, B = 25 µg/ml, C = 50 µg/ml, and D = 100 µg/ml). FL2H is the norm filter of the flow cytometer.

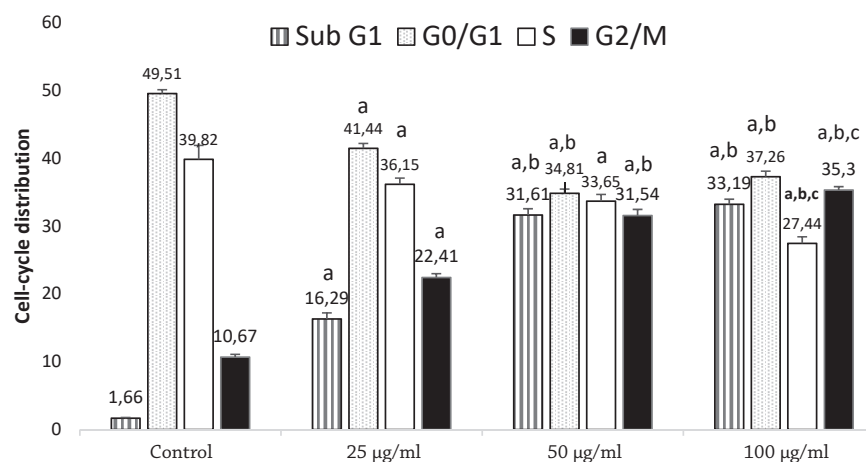


Fig. 4. Cell-cycle distribution of HepG-2 cells treated with the *H. cuneiformis* extract at different concentrations (25, 50, and 100 µg/ml), compared to the untreated control. DNA was stained with propidium iodide and analyzed by flow cytometry. The data presents the mean of 3 replicas ± S.D. **a:** significant difference as compared to control, **b:** compared to 25 µg/ml of extract, and **c:** compared to 50 µg/ml of the extract. $P \leq 0.05$ was accepted as a significant difference.

Annexin V analysis

To determine apoptosis and necrosis percentage upon extract treatment, annexin V assay was applied (Fig. 5). The results reflect a significant increase in early, late, and total apoptosis, as well as necrosis, concentration-dependently (Fig. 6). The 100 µg/ml concentration recorded 11.4% necrosis compared to 1.04% necrosis for the low dose. Early and late apoptosis

increased from 0.51% and 0.11% in the control to 7.67% and 18.58% in the 100 µg/ml extract concentration, respectively. Total apoptosis increased from 1.56% in the control to 30.01% in the 100 µg/ml extract concentration. The results indicate that a decrease in cancer cell proliferation is more likely due to the triggering of apoptosis rather than necrosis, which confirms the cell cycle results.

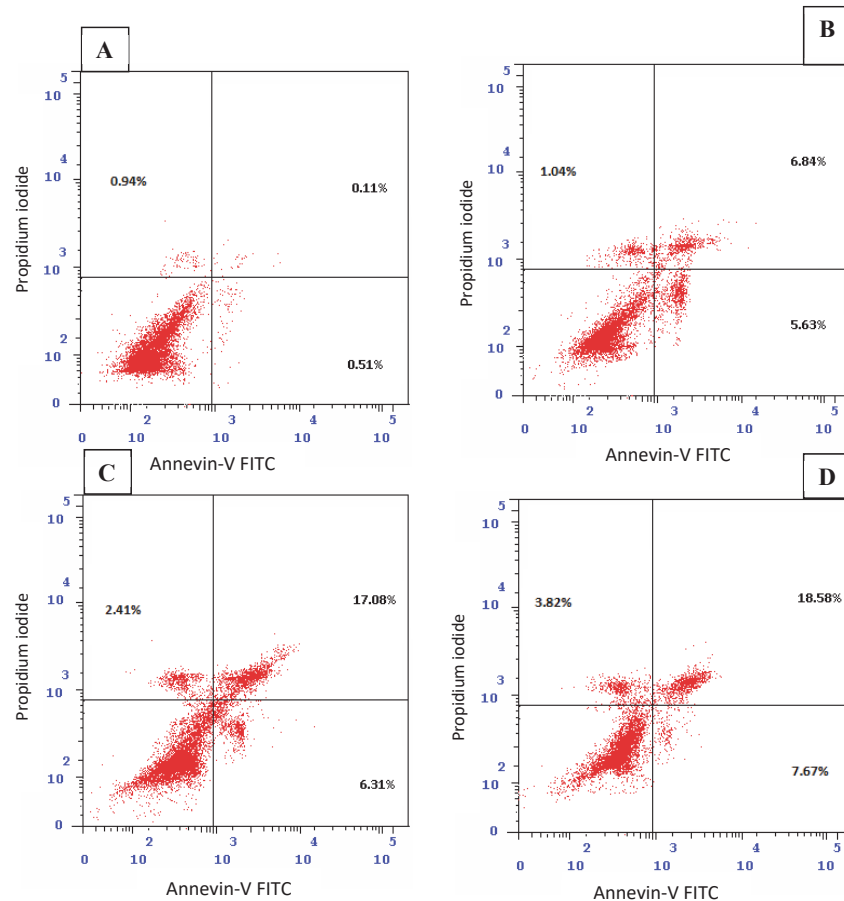


Fig. 5. The proportion of apoptotic HepG-2 cells evaluated via the annexin-V flow cytometry assay using different extract concentrations versus control untreated cells (**A** = control, **B** = 25 µg/ml, **C** = 50 µg/ml and **D** = 100 µg/ml)

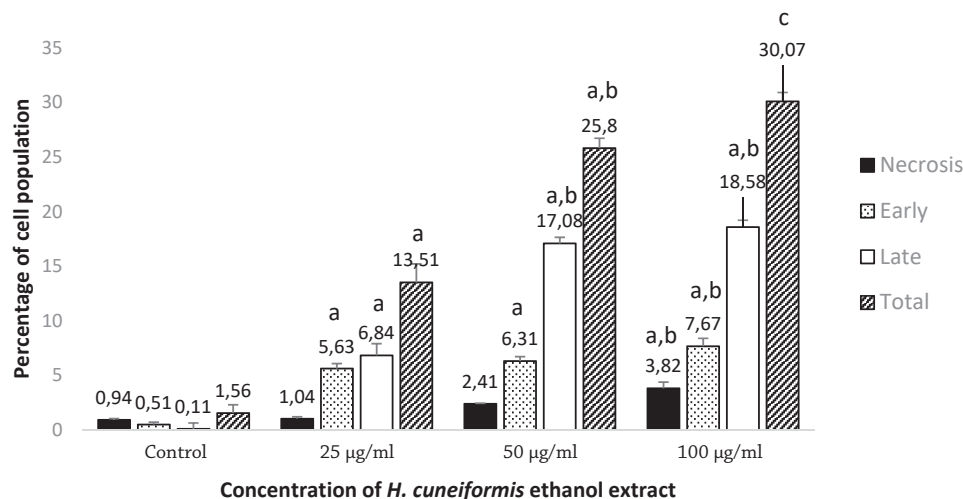


Fig. 6. The effect of the *H. cuneiformis* ethanol extract at different concentrations (25, 50, and 100 µg/ml) on apoptosis induction stages (necrosis, early apoptosis, late apoptosis, and total apoptosis) in HepG-2 cells compared to control (untreated cells). Values are presented as means ± S.D ($n = 3$). Columns carrying different letters are significantly different from each other. $P \leq 0.05$ was accepted as a significant difference.

Oxidative status biomarkers

To examine the oxidative status of cancer cells before and after extract treatment, the enzymatic and non-enzymatic antioxidants were measured (Table 5). MDA is a byproduct of the lipid peroxidation (LPO) process and an indicator of damage (Pradhan et al., 2021; Zhang et al., 2012). The results showed a significant elevation of MDA levels from 14.58 ± 0.57 to 63.89 ± 0.82 nmol/ml in control and 100 µg/ml treatments, respectively. A concentration-dependent increase in MDA reveals the extract's ability to harm cancer cells. This result agreed with that of Yusof and Abdul-Aziz (2005), who studied the anticancer effect of ginger extract on HepG-2 cells. MPO is an enzyme related to the immune response of the host. According to the current results, MPO was found to increase

from 15.24 ± 0.11 (control) to 19.3 ± 0.76 (100 µg/ml) U/ml. This result was in agreement with Ali et al. (2022), who suggested the increase of MPO as a modern procedure of anticancer treatment, especially for radiotherapy patients.

The results reveal a rise in the antioxidant enzymes and non-enzyme CAT, GST, and GSH (Table 5). SOD levels have been found to significantly rise at the extract's concentration of 25 g/ml while falling at the 100 g/ml level. The extract did not show a significant effect on GPx. These results were in agreement with Zhang et al. (2012), who studied the effect of aqueous extract of *Sargassum pallidum* in gastric cancer. The results were also in agreement with Popovici et al. (2021) who studied the effect of *Usnea barbata* extract on the oxidative status of oral carcinoma.

Table 5. Evaluation of the effect of different extract concentrations of algae on the antioxidant enzymes of HepG-2 cells

Oxidative-antioxidant parameters	Control	Treated (µg/ml)		
		25	50	100
MDA (nmol/ml)	$14.58^d \pm 0.57$	$36.41^c \pm 0.73$	$62.13^b \pm 0.62$	$63.89^a \pm 0.82$
MPO (U/ml)	$15.24^c \pm 0.11$	$15.06^{c+d} \pm 0.9$	$18.99^b \pm 0.93$	$19.3^a \pm 0.76$
SOD (U/mg proteins)	$4.91^c \pm 0.41$	$5.0^a \pm 0.56$	$4.96^b \pm 0.9$	$4.89^c \pm 0.5$
CAT (U/mg proteins)	$3.14^d \pm 0.05$	$3.23^c \pm 0.41$	$3.44^b \pm 0.56$	$3.52^a \pm 0.9$
GPx (U/mg proteins)	$2.64^a \pm 0.11$	$2.25^d \pm 0.21$	$2.46^c \pm 0.54$	$2.53^{a+b} \pm 0.76$
GST (nmol/mg proteins)	$3.03^d \pm 0.21$	$3.09^c \pm 0.54$	$3.11^b \pm 0.57$	$3.27^a \pm 0.62$
GSH (µmol/mg proteins)	$0.31^b \pm 0.03$	$0.25^c \pm 0.01$	$0.3^b \pm 0.01$	$0.32^a \pm 0.01$

Note: The data is presented as mean \pm S.E ($n = 3$). MDA, malondialdehyde; MPO, myeloperoxidase; SOD, superoxide dismutase; CAT, catalase; GPx, glutathione peroxidase; GST, glutathione-S-transferase; and GSH, glutathione. $P \leq 0.05$ was accepted as a significant difference. The same raw values with different letters are significantly different.

This research demonstrates that *H. cuneiformis* extracts have anticancer properties due to the induction of oxidative stress and antioxidant enzyme imbalance, which induce cytotoxicity in the cancer cells. The results were different from other studies, which suggest that the anticancer activity of some natural extracts is due to the antioxidant protective effect of lowering GSH, MDA, and MPO, while increasing SOD, CAT, and GPx (Su et al., 2014). The contradiction between studies may be due to the difference in both cancer cells and extract behaviors. As there are no previous studies on the effect of *H. cuneiformis* extract on the oxidative status of HepG-2 cells (to the best of the authors' knowledge), more studies are required to understand the triggered signal pathways for the extract.

Transmission electron microscopy (TEM)

TEM was used to examine the morphological ultra-microstructural alterations in HepG-2 cancer cells after treatment with an IC50 concentration of the extract compared to control untreated cells (Figs 7, 8). According to the TEM images, the morphological changes in the treated cells (Fig. 8) compared to the control (Fig. 7) included cell membrane blebbing, microvilli absence/reduction (blunt microvillus), chromatin aggregation, mitochondrial denaturation, apoptotic body formation, and lysosomes containing analytic organelles. Also, it shows cytoplasmic compartments, swelling, and mitochondrial cristate disappearances. The findings confirmed that the extract can induce apoptosis. These actions toward cancer cell morphology have been reported for other marine macroalgal extracts (Namvar et al., 2013).

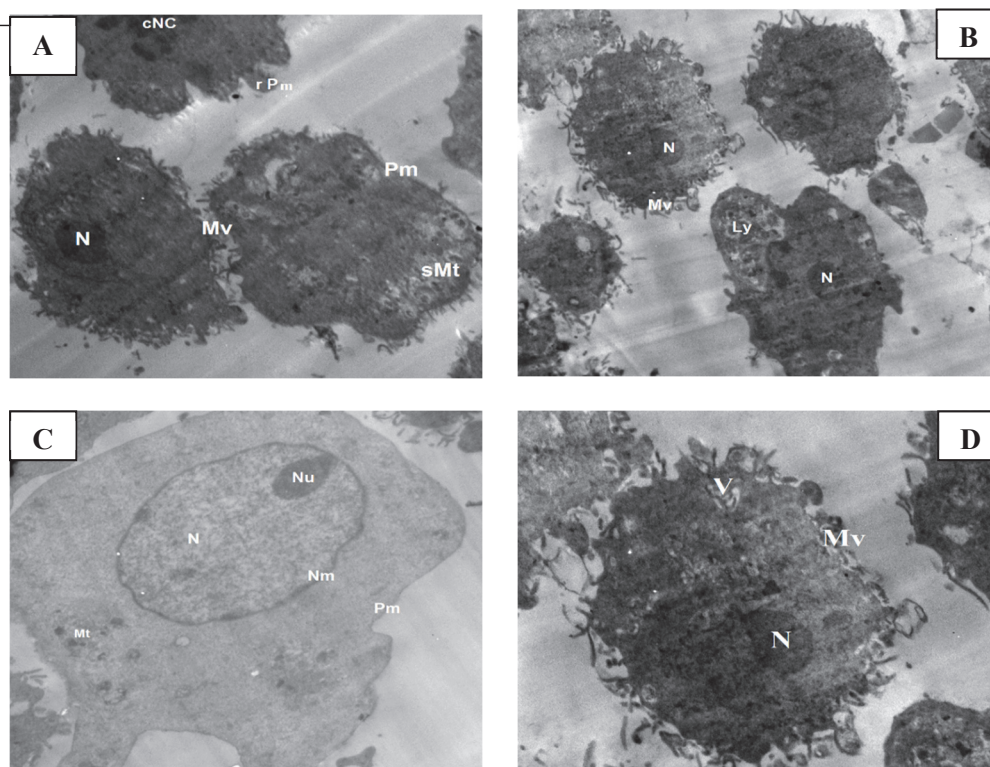


Fig. 7. Transmission electron microscopy (TEM) of the positive control HepG-2 cell line. **A–B** shows a magnification of 5000 \times ; **C** shows a magnification of 8000 \times ; and **D** shows a high magnification at 10,000 \times . cNC, condensed nuclear chromatin; Ly, lysosomes; Mt, mitochondria; Mv, microvilli; N, nuclei; Nm, nuclear membrane; Nu, nucleoli; Pm, plasma membrane; rPm, rounded plasma membrane; sMt, swelling mitochondria; V, vacuole.

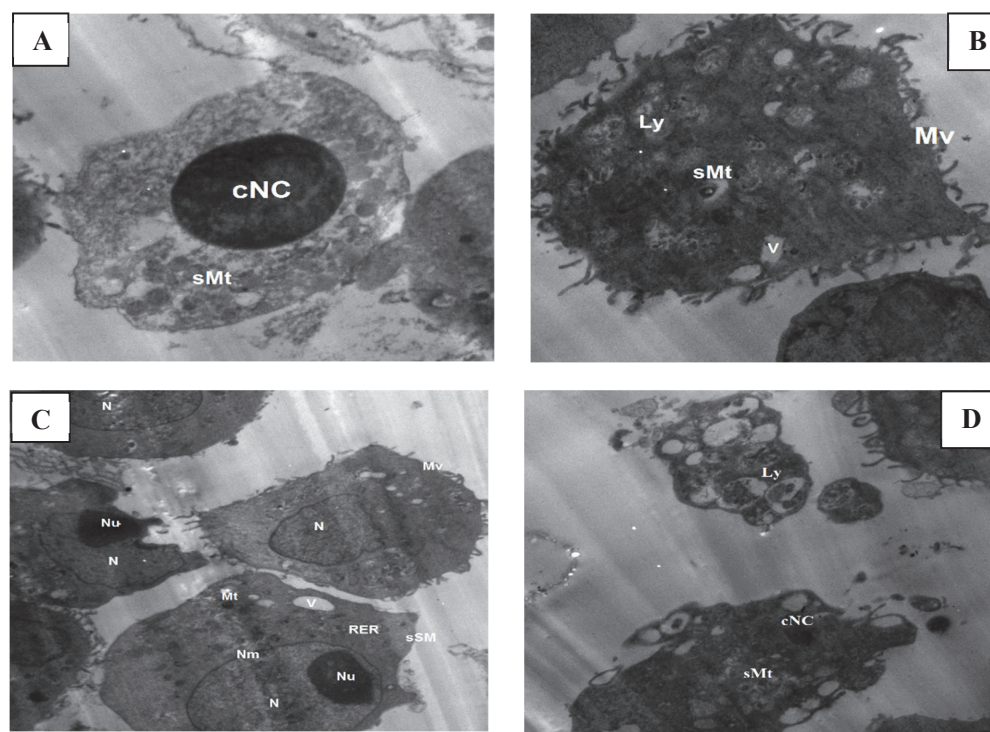


Fig. 8. Transmission electron microscopy (TEM) of the HepG-2 cell line after treatment with IC₅₀ (44.6 μ g/ml) of the *H. cuneiformis* extract. **A–B** show high magnification at 10,000 \times ; **C** shows magnification at 5000 \times ; **D** shows magnification at 8000 \times . cNC, condensed nuclear chromatin; Ly, lysosomes; Mt, mitochondria; Mv, microvilli; N, nucleus; Nm, nuclear membrane; Nu, nucleoli; RER, rough endoplasmic reticulum; sMt, swelling mitochondria; sSM, smooth surface membrane; V, vacuole.

Conclusion

The goal of the present study was to examine the chemical composition, antibacterial, and anticancer properties of the ethanol extract of *H. cuneiformis*. The study clarifies that fatty acids, which have previously been noted for their antibacterial and anticancer effects, are the predominant components in the chemical profile of *H. cuneiformis*. The extract was proven to possess a broad-spectrum antimicrobial effect through the growth suppression of *E. coli*, *S. aureus*, *B. subtilis*, and *C. albicans* in a comparable manner to commercial antibiotics. The normal Vero cells were found to be well adapted to the extract concentrations with slight cytotoxicity towards the 500 µg/ml concentration. The three cancer cell lines under investigation showed that the extract has anticancer action. (MCF-7, HepG-2, and HEP-2) in correlation to the concentration with the highest cytotoxicity against HepG-2, which was chosen for further investigations. The cytotoxic mechanism of the extract was found to be related to apoptosis and cell cycle arrest through the increase of sub-G1 and G2-M phases in comparison to the control. This result was confirmed with Annexin V analysis of apoptosis, which showed a concentration-correlated increase in total apoptosis (as a percentage). The extract induces oxidative stress in HepG-2 cancer cells as evidenced by the increased levels of MDA and MPO. The effect on GSH levels depends on the concentration of the extract, with a decrease observed at a low concentration (25 µg/ml). However, the extract appears to enhance the activities of CAT, GPx, and GST, which are antioxidant enzymes at higher concentrations. The decrease in SOD activity suggests a potential impairment in the cell's ability to neutralize superoxide radicals. Overall, these results suggest that the extract may exert its cytotoxic effects on cancer cells by inducing oxidative stress and disrupting the balance of antioxidant enzymes.

The observation of apoptotic body formation in treated cells suggests that the *H. cuneiformis* extract contains bioactive compounds with potential antimicrobial and anticancer properties. Further research is needed to isolate, purify, identify, and understand the mode of action of these compounds before they can be considered for drug development.

Author contributions

All the authors have read and agreed to the published version of the manuscript.

Conflict of interest

The authors have no conflict of interest to declare.

Acknowledgment and funding

The researchers would like to acknowledge the Deanship of Scientific Research, Taif University, for funding this work.

In cooperation with Suez Canal University, Ismailia, Egypt.

References

- Abbas Z, Rehman S (2018). An overview of cancer treatment modalities. *Neoplasm* 1: 139–157. DOI: 10.5772/intechopen.76558.
- Abubakar MN, Majinda RRT (2016). GC-MS analysis and preliminary antimicrobial activity of *Albizia adianthifolia* (Schumacher) and *Pterocarpus angolensis* (DC). *Medicines*, 3(1): 3. DOI: 10.3390/medicines3010003.
- Agoramoorthy G, Chandrasekaran M, Venkatesalu V, Hsu MJ (2007). Antibacterial and antifungal activities of fatty acid methyl esters of the blind-your-eye mangrove from India. *Braz J Microbiol* 38(4): 739–742. DOI: 10.1590/S1517-83822007000400028.
- Akpuaka A, Ekwenchi MM, Dashak DA, Dildar A (2013). Biological activities of characterized isolates of n-hexane extract of *Azadirachta indica* A. Juss (Neem) leaves. *J Nat Sci* 11(5): 141–147.
- Ali M, Fulci G, Grigalavicius M, Pulli B, Li A, Wojtkiewicz GR, et al. (2022). Myeloperoxidase exerts anti-tumor activity in glioma after radiotherapy. *Neoplasm* 26: 100779. DOI: 10.1016/j.neo.2022.100779.
- Arguelles EDLR, Sapin AB (2022). Proximate composition and *in vitro* analysis of antioxidant and antibacterial activities of *Padina boryana* Thivy. *Sci Eng Health Stud* 16: 22030002. DOI: 10.14456/sehs.2022.2.
- Barreca M, Spanò V, Montalbano A, Cueto M, Díaz Marrero AR, Deniz I, et al. (2020). Marine anticancer agents: An overview with a particular focus on their chemical classes. *Mar Drugs* 18(12): 619. DOI: 10.3390/md18120619.
- Barzkar N, Tamadoni Jahromi S, Poorsaheli HB, Vianello F (2019). Metabolites from marine microorganisms, micro, and macroalgae: Immense scope for pharmacology. *Mar Drugs* 17(8): 464. DOI: 10.3390/md17080464.
- Belakhdar G, Benjouad A, Abdennebi EH (2015). Determination of some bioactive chemical constituents from *Thesium humile* Vahl. *J Mater Environ Sci* 6(10): 2778–2783.
- Behravan M, Panahi AH, Naghizadeh A, Ziaee M, Mahdavi R, Mirzapour A (2019). Facile green synthesis of silver nanoparticles using *Berberis vulgaris* leaf and root aqueous extract and its antibacterial activity. *Int J Biol Macromol* 124: 148–154. DOI: 10.1016/j.ijbiomac.2018.11.101.
- Berry MF (2014). Esophageal cancer: Staging system and guidelines for staging and treatment. *J Thorac Dis* 6(Suppl. 3), S289–297. DOI: 10.3978/j.issn.2072-1439.2014.03.11.
- Beulah GG, Soris PT, Mohan VR (2018). GC-MS Determination of Bioactive Compounds of *Dendrophthoe falcata* (LF) Ettingsh: An Epiphytic Plant. *Int J Health Sci Res* 8(11): 261–269.
- Biris-Dorhoi ES, Michiu D, Pop CR, Rotar AM, Tofana M, Pop OL, et al. (2020). Macroalgae – A sustainable source of chemical compounds with biological activities. *Nutrients* 12(10): 3085. DOI: 10.3390/nu12103085.
- Chamberlin SR, Blucher A, Wu G, Shinto L, Choonoo G, Kulesz-Martin M, McWeeney S (2019). Natural product target network reveals potential for cancer combination therapies. *Front Pharmacol* 10: 557. DOI: 10.3389/fphar.2019.00557.
- Chojnacka K, Saeid A, Witkowska Z, Tuhy L (2012). Biologically active compounds in seaweed extracts – the prospects for the application. *Open Conf Proc J* 3(1). DOI: 10.2174/1876326X01203020020.
- Claiborne A (1985). Handbook of methods for oxygen radical research. Florida: Chemical Rubber Company (CRC) Press, Boca Raton, 2 p.
- Crout RJ, Gilbertson JR, Gilbertson JD, Platt D, Langkamp HH, Connacher RH (1982). Effect of linolenyl alcohol on the *in-vitro* growth of the oral bacterium *Streptococcus mutans*. *Arch Oral Biol* 27(12): 1033–1037. DOI: 10.1016/0003-9969(82)90008-5.
- El-Din SMM, Mohyeldin MM (2018). Component analysis and antifungal activity of the compounds extracted from four brown seaweeds with different solvents at different seasons. *J Ocean Univ China* 17(5): 1178–1188. DOI: 10.1007/s11802-018-3538-2.
- El Shafay SM, Ali SS, El-Sheekh MM (2016). Antimicrobial activity of some seaweeds species from Red Sea, against multidrug resistant bacteria. *Egypt J Aquat Res* 42(1): 65–74. DOI: 10.1016/j.ejar.2015.11.006.
- Ellman GL (1959). Tissue sulfhydryl groups. *Arch Biochem Biophys* 82(1): 70–77. DOI: 10.1016/0003-9861(59)90090-6.
- Elsayed TR, Galil DE, Sedik MZ, Hassan HMM, Gohar MR, Sadik MW (2020). Antimicrobial and Anticancer Activities of Actinomycetes Isolated from Egyptian Soils. *Int J Curr Microbiol App Sci* 9(9). DOI: 10.20546/ijcmas.2020.909.209.
- Gideon VA (2015). GC-MS analysis of phytochemical components of *Pseudoglochidion anamalayanum* Gamble: an endangered medicinal tree. *Asian J Plant Sci Res* 5(12): 36–41.

- Graham L, Orenstein JM (2007). Processing tissue and cells for transmission electron microscopy in diagnostic pathology and research. *Nat Protoc* 2(10): 2439–2450. DOI: 10.1038/nprot.2007.304.
- Guerrero RV, Abarca-Vargas R, Petricevich VL (2017). Chemical compounds and biological activity of an extract from *Bougainvillea x buttiana* (var. Rose) Holttum and Standl. *Int J Pharm Pharm Sci* 9(3): 42–46. DOI: 10.22159/ijpps.2017v9i3.16190.
- Gupta S, Abu-Ghannam N (2011). Bioactive potential and possible health effects of edible brown seaweeds. *Trends Food Sci Technol* 22(6): 315–326. DOI: 10.1016/j.tifs.2011.03.011.
- Gutiérrez-Rodríguez AG, Juárez-Portilla C, Olivares-Bañuelos T, Zepeda RC (2018). Anticancer activity of seaweeds. *Drug Discov Today* 23(2): 434–447. DOI: 10.1016/j.drudis.2017.10.019.
- Ibrahim HAH, Elshaer MM, Elatriby DE, Ahmed HO (2020). Antimicrobial activity of the sea star (*Astropecten spinulosus*) collected from the Egyptian Mediterranean Sea, Alexandria. *Egypt J Aquat Biol Fish* 24(2): 507–523. DOI: 10.21608/ejabf.2020.86046.
- Jargalsaikhan U, Javzan S, Selenge D, Nedelcheva D, Philipov S, Nadmid J (2014). Fatty acids and their esters from *Cicuta virosa* L. *Mong J Chem* 14: 71–74. DOI: 10.5564/mjc.v14i0.203.
- Kajstura M, Halicka HD, Pryjma J, Darzynkiewicz Z (2007). Discontinuous fragmentation of nuclear DNA during apoptosis revealed by discrete “sub-G1” peaks on DNA content histograms. *Cytometry A* 71(3): 125–131. DOI: 10.1002/cyto.a.20357.
- Kim BR, Kim HM, Jin CH, Kang SY, Kim JB, Jeon YG, et al. (2020). Composition and Antioxidant Activities of Volatile Organic Compounds in Radiation-Bred *Coreopsis* Cultivars. *Plants* 9(6): 717. DOI: 10.3390/plants9060717.
- Küçük HB, Yusufoglu A, Mataracı E, Döşler S (2011). Synthesis and biological activity of new 1, 3-dioxolanes as potential antibacterial and antifungal compounds. *Molecules*, 16(8): 6806–6815. DOI: 10.3390/molecules16086806.
- Lakshmanan I, Batra SK (2013). Protocol for apoptosis assay by flow cytometry using annexin V staining method. *Bio Protoc* 3(6): e374. DOI: 10.21769/bioprotoc.374.
- Malathi K, Ramaiah S (2017). Ethyl iso-allocholate from a medicinal rice *Karunkavuni* inhibits dihydropteroate synthase in *Escherichia coli*: A molecular docking and dynamics study. *Indian J Pharm Sci* 78(6): 780–788. DOI: 10.4172/pharmaceutical-sciences.1000184.
- Marimuthu K, Nagaraj N, Ravi O (2014). GC-MS analysis of phytochemicals, fatty acids, and antimicrobial potency of dry *Christmas lima* beans. *Int J Pharm Sci Rev Res* 27(2): 63–66.
- Marklund SL (1985). Pyrogallol autooxidation. *Handbook of Methods for Oxygen Radical Research*, 6 p.
- Mirabelli P, Coppola L, Salvatore M (2019). Cancer cell lines are useful model systems for medical research. *Cancers* 11(8): 1098. DOI: 10.3390/cancers11081098.
- Moga MA, Dima L, Balan A, Blidaru A, Dimienescu OG, Podasca C, Toma S (2021). Are bioactive molecules from seaweeds a novel and challenging option for the prevention of HIV infection and cervical cancer therapy? A review. *Int J Mol Sci* 22(2): 629. DOI: 10.3390/ijms22020629.
- Mohamed SS, Saber AA (2019). Antifungal potential of the bioactive constituents in extracts of the mostly untapped brown seaweed *Hormophysa cuneiformis* from the Egyptian coastal waters. *Egypt J Bot* 59(3): 695–708. DOI: 10.21608/ejbo.2019.5516.1225.
- Monzote L, García M, Montalvo AM, Scull R, Miranda M (2010). Chemistry, cytotoxicity and antileishmanial activity of the essential oil from *Piper auritum*. *Mem Inst Oswaldo Cruz* 105(2): 168–173. DOI: 10.1590/s0074-02762010000200010.
- Mosmann T (1983). Rapid colorimetric assay for cellular growth and survival: Application to proliferation and cytotoxicity assays. *J Immunol Methods* 65(1–2): 55–63. DOI: 10.1016/0022-1759(83)90303-4.
- Mujeeb F, Bajpai P, Pathak N (2014). Phytochemical evaluation, antimicrobial activity, and determination of bioactive components from leaves of *Aegle marmelos*. *Biomed Res Int* 2014: 497606. DOI: 10.1155/2014/497606.
- Mushtaq A, Rasool N, Riaz M, Tareen RB, Zubair M, Rashid U, et al. (2013). Antioxidant, Antimicrobial studies and characterization of essential oil, fixed oil of *Clematis graveolens* by GC-MS. *Oxid Commun* 36(4): 1067–1078.
- Namvar F, Mohamad R, Baharara J, Zafar-Balanejad S, Fargahi F, Rahman HS (2013). Antioxidant, antiproliferative, and antiangiogenesis effects of polyphenol-rich seaweed (*Sargassum muticum*). *Biomed Res Int* 2013: 604787. DOI: 10.1155/2013/604787.
- Nicoletti I, Migliorati G, Pagliacci MC, Grignani F, Riccardi C (1991). A rapid and simple method for measuring thymocyte apoptosis by propidium iodide staining and flow cytometry. *J Immunol Methods* 139(2): 271–279. DOI: 10.1016/0022-1759(91)90198-o.
- Nishanthini A, Mohan VR, Jeeva S (2014). Phytochemical, FT-IR, and GC-MS analysis of stem and leaf of *Tiliacora acuminata* (Lan.) Hook F & Thomas (Menispermaceae). *Int J Pharm Sci Res* 5(9): 3977–3986. DOI: 10.13040/IJPSR.0975-8232.5(9).3977-86.
- Osman NA, Siam AA, El-Manawy I, Jeon YJ (2019). Anti-microbial and anti-diabetic activity of six seaweeds collected from the Red Sea, Egypt. *Catrina J* 19(1): 55–60. DOI: 10.21608/cat.2019.49157.
- Osman NA, Siam A, M El-Manawy I, Jeon YJ (2020). Anticancer activity of a scarcely investigated red sea brown alga *Hormophysa cuneiformis* against HL60, A549, HCT116, and B16 cell lines. *Egypt J Aquat Biol Fish* 24(1): 497–508. DOI: 10.21608/ejabf.2020.75087.
- Pádua D, Rocha E, Gargiulo D, Ramos AA (2015). Bioactive compounds from brown seaweeds: phloroglucinol, fucoxanthin, and fucoidan as promising therapeutic agents against breast cancer. *Phytochem Lett* 14: 91–98. DOI: 10.1016/j.phytol.2015.09.007.
- Paglia DE, Valentine WN (1967). Studies on the quantitative and qualitative characterization of erythrocyte glutathione peroxidase. *J Lab Clin Med* 70(1): 158–169.
- Parham S, Kharazi AZ, Bakhsheshi-Rad HR, Nur H, Ismail AF, Sharif S, et al. (2020). Antioxidant, antimicrobial, and antiviral properties of herbal materials. *Antioxidants* 9(12): 1309. DOI: 10.3390/antiox9121309.
- Pinteus S, Silva J, Alves C, Horta A, Thomas OP, Pedrosa R (2017). Antioxidant and cytoprotective activities of *Fucus spiralis* seaweed on a human cell *in vitro* model. *Int J Mol Sci* 18(2): 292. DOI: 10.3390/ijms18020292.
- Pasaribu G, Waluyo TK (2020). Ethnomedicine, phytochemical, and toxicity activity of several alleged medicinal plants from Sebangau National Park, Central Borneo. *IOP Conf. Ser: Earth Environ Sci* 415 012007. DOI: 10.1088/1755-1315/415/1/012007.
- Piroux E, Caty G, Aboubakar Nana F, Reyckler G (2020). Effects of exercise therapy in cancer patients undergoing radiotherapy treatment: A narrative review. *SAGE Open Medicine* 8: 2050312120922657. DOI: 10.1177/2050312120922657.
- Popovici V, Bucur L, Vochita G, Gherghel D, Mihai CT, Rambu D, et al. (2021). *In vitro*, anticancer activity and oxidative stress biomarkers status determined by *Usnea barbata* (L.) FH Wigg. dry extracts. *Antioxidants* 10(7): 1141. DOI: 10.3390/antiox10071141.
- Pradhan B, Nayak R, Patra S, Jit BP, Ragusa A, Jena M (2021). Bioactive metabolites from marine algae as potent pharmacophores against oxidative stress-associated human diseases: A comprehensive review. *Molecules* 26(1): 37. DOI: 10.3390/molecules26010037.
- Rashad S, El-Chaghaby G (2020). Marine algae in Egypt: distribution, phytochemical composition and biological uses as bioactive resources (a review). *Egypt J Aquat Biol Fish* 24(5): 147–160. DOI: 10.21608/ejabf.2020.103630.
- Rayssan R, Shawkat MS (2019). Cytotoxicity Assessment of *Malva sylvestris* Crude Extract on Melanoma and Lymphoma Cell Lines. *J Pharm Sci Res* 11(1): 70–74.
- Reddy DN, Al-Rajab AJ (2016). Chemical composition, antibacterial and antifungal activities of *Ruta graveolens* L. volatile oils. *Cogent Chem* 2(1): 1220055. DOI: 10.1080/23312009.2016.1220055.
- Rency RC, Vasanthak K, Maruthasalam A (2015). Identification of bioactive compounds from ethanolic leaf extracts of *Premna serratifolia* L. using GC-MS. *Biosci Discov* 6(2): 96–101.
- Sakthivel R, Devi KP (2019). Antioxidant, anti-inflammatory, and anticancer potential of natural bioactive compounds from

- seaweeds. *Stud Nat Prod Chem* 63: 113–160. DOI: 10.1016/B978-0-12-817901-7.00005-8.
- Salehi B, Sharifi-Rad J, Seca AML, Pinto DCGA, Michalak I, Trincone A, et al. (2019). Current trends on seaweeds: looking at chemical composition, phytopharmacology, and cosmetic applications. *Molecules* (Basel, Switzerland) 24(22): 4182. DOI: 10.3390/molecules24224182.
- Seca AML, Pinto D (2018). Plant secondary metabolites as anticancer agents: Successes in clinical trials and therapeutic application. *Int J Mol Sci* 19(1). DOI: 10.3390/ijms19010263.
- Seyyedi MA, Farahnak A, Jalali M, Rokni MB (2005). Study on Glutathione S-transferase (GST) inhibition assay by triclabendazole. I: Protoscoleces (Hydatid Cyst; *Echinococcus granulosus*) and Sheep Liver Tissue. *Iran J Public Health* 34(1): 38–46.
- Shukla S, Hegde S, Kumar A, Chaudhary G, Tewari SK, Upreti DK, Pal M (2018). Fatty acid composition and antibacterial potential of *Cassia tora* (leaves and stem) collected from different geographic areas of India. *J Food Drug Anal* 26(1): 107–111. DOI: 10.1016/j.jfda.2016.12.010.
- Sianipar NF, Purnamaningsih R (2016). Bioactive compounds of fourth generation gamma-irradiated *Typhonium flagelliforme* Lodd. mutants based on gas chromatography-mass spectrometry. *IOP Conf. Ser.: Earth Environ Sci* 41 012025. DOI: 10.1088/1755-1315/41/1/012025.
- Silva A, Silva SA, Lourenço-Lopes C, Jimenez-Lopez C, Carpena M, Gullón P, et al. (2020). Antibacterial use of macroalgae compounds against foodborne pathogens. *Antibiotics* 9(10): 712. DOI: 10.3390/antibiotics9100712.
- Su ZQ, Mo ZZ, Liao JB, Feng XX, Liang YZ, Zhang X, et al. (2014). Usnic acid protects LPS-induced acute lung injury in mice through attenuating inflammatory responses and oxidative stress. *Int Immunopharmacol* 22(2): 371–378. DOI: 10.1016/j.intimp.2014.06.043.
- Teixeira TR, Santos GSD, Armstrong L, Colepicolo P, Debonsi HM (2019). Antitumor Potential of Seaweed Derived-Endophytic Fungi. *Antibiotics* 8(4): 205. DOI: 10.3390/antibiotics8040205.
- Teleb WK, Tantawy MA, Osman NA, Abdel-Rahman MA, Hussein AA (2022). Structural and cytotoxic characterization of the marine red algae *Sarconema filiforme* and *Laurencia obtusa*. *Egypt J Aquat Biol Fish* 26(4): 549–573. DOI: 10.21608/ejabf.2022.252760.
- Țigu AB, Moldovan CS, Toma VA, Farcaș AD, Moț AC, Jurj A, et al. (2021). Phytochemical analysis and *in vitro* effects of *Allium fistulosum* L. and *Allium sativum* L. extracts on human normal and tumor cell lines: A comparative study. *Molecules* 26(3): 574. DOI: 10.3390/molecules26030574.
- Tyagi T, Agarwal M (2017). Phytochemical and GC-MS analysis of bioactive constituents in the ethanolic of *Pistia stratiotes* L. and *Eichhornia crassipes* (Mart.) solms. *J Pharmacogn Phytochem* 6(1): 195–206.
- Uchiyama M, Mihara M (1978). Determination of malonaldehyde precursor in tissues by thiobarbituric acid test. *Anal Biochem* 86(1): 271–278. DOI: 10.1016/0003-2697(78)90342-1.
- Vijayarathna S, Sasidharan S (2012). Cytotoxicity of methanol extracts of *Elaeis guineensis* on MCF-7 and Vero cell lines. *Asian Pac J Trop Biomed* 2(10): 826–829. DOI: 10.1016/S2221-1691(12)60237-8.
- Wang CZ, Luo Y, Huang WH, Zeng J, Zhang CF, Lager M, et al. (2021). Falcariindiol and dichloromethane fraction are bioactive components in *Oplopanax elatus*: Colorectal cancer chemoprevention via induction of apoptosis and G2/M cell cycle arrest mediated by cyclin A upregulation. *J Appl Biomed* 19(2): 113–124. DOI: 10.32725/jab.2021.013.
- WHO (2021). Antimicrobial resistance. [online] [cit. 2023-01-22]. Available from: <https://www.who.int/news-room/fact-sheets/detail/antimicrobial-resistance>
- WHO (2022). Cancer. [online] [cit. 2023-01-22]. Available from: <https://www.who.int/news-room/fact-sheets/detail/cancer>
- Yusof Yam, Abdul-Aziz A (2005). Effects of *Zingiber officinale* on superoxide dismutase, glutathione peroxidase, catalase, glutathione, and malondialdehyde content in HepG2 cell line. *Malaysian J Biochem Mol Biol* 11: 36–41.
- Yuyama KT, Rohde M, Molinari G, Stadler M, Abraham WR (2020). Unsaturated fatty acids control biofilm formation of *Staphylococcus aureus* and other gram-positive bacteria. *Antibiotics* 9(11): 788. DOI: 10.3390/antibiotics9110788.
- Zayed MZ, Ahmad FB, Ho WS, Pang SL (2014). GC-MS analysis of phytochemical constituents in leaf extracts of *Neolamarckia cadamba* (Rubiaceae) from Malaysia. *Int J Pharm Pharm Sci* 6(9): 123–127.
- Zhang RL, Luo WD, Bi TN, Zhou SK (2012). Evaluation of antioxidant and immunity-enhancing activities of *Sargassum pallidum* aqueous extract in gastric cancer rats. *Molecules* 17(7): 8419–8429. DOI: 10.3390/molecules17078419.
- Zorofchian Moghadamtousi S, Karimian H, Khanabdali R, Razavi M, Firoozinia M, Zandi K, Abdul Kadir H (2014). Anticancer and antitumor potential of fucoidan and fucoxanthin, two main metabolites isolated from brown algae. *Sci World J* 2014: 768323. DOI: 10.1155/2014/768323.